J. Mater. Environ. Sci. 4(6) (2013) 921-930
ISSN : 2028-2508
CODEN: JMESCN

Comparative inhibition study of mild steel corrosion in hydrochloric acid by benzimidazole derivatives

R. Touir[1,*], R. A. Belakhmima[1], M. Ebn Touhami[1], L. Lakhrissi[2.3], M. El Fayed[2], B. Lakhrissi[2], E. M. Essassi[3]

[1] *laboratoire de Matériaux, Electrochimie et Environnement, Université Ibn Tofail, Faculté des Sciences, BP 133, Kénitra, Maroc*
[2]*Laboratoire d'Agroressources et Génie des Procédés, Université Ibn Tofail, Faculté des Sciences, Kénitra, Maroc*
[3]*Laboratoire de Chimie Organique Hétérocyclique, Université Mohammed V - Agdal , Faculté des Sciences, Rabat, Maroc*

Received 22 Jan 2013, Revised 8 July 2013, Accepted 8 July 2013
* Corresponding author. Tel.: + 212 670 52 69 59; *Email address*: touir8@yahoo.fr

Abstract
The 5-chloro-benzimidazol-2-one (B1), 5-methyl-benzimidazol-2-one (B2) and benzimidazol-2-one (B3) have been investigated for mild steel corrosion in 1 M HCl at different concentrations using weight loss measurements, potentiodynamic polarization curves and electrochemical impedance spectroscopy (EIS) methods. Generally, inhibition efficiency of the investigated compounds was found to depend on inhibitor concentration and their structures. A comparison results showed that B1 was the best inhibitor. For this, a detailed study was making for this compound using electrochemical measurements. Potentiodynamic polarization studies clearly reveal that B1 acts essentially as mixed inhibitor. The inhibition efficiency increases with immersion time and concentration. In addition, at 24 h, the EIS showed the formation of a protective film. The adsorption of B1 on mild steel surface is found to obey Langmuir adsorption isotherm.

Key words: Benzimidazole derivatives; Mild steel; Hydrochloric acid; Corrosion inhibition.

1. Introduction:
Corrosion problems have received a considerable amount of attention because of their attack on materials. Due to its prominent properties, hydrochloric acid is widely used in industry, for example, acid pickling, acid cleaning and acid descaling. The use of inhibitors is one of the most practical methods for protection against corrosion. The metals corrosion inhibition in acids by organic additives has been studied in considerable detail [1–4].
Most of the efficient inhibitors used in industry are organic compounds which mainly contain oxygen, sulphur, nitrogen atoms and multiple bonds in the molecule through which they are adsorbed on metal surface [5–8]. Moreover, many *N*-heterocyclic compounds have been proved to be effective inhibitors for metals and alloys corrosion in aqueous media [9–13].
This paper is aimed to determine the inhibition efficiency of benzimidazole derivatives via mild steel corrosion in 1 M HCl solution at different concentration in order to compare their effect molecular structure. The effect of concentration and immersion time of the best inhibitor using electrochemical measurements was evaluated and discussed.

2. Experimental details:
The formulas structures of 5-chloro-benzimidazol-2-one (B1), 5-methyl-benzimidazol-2-one (B2) and benzimidazol-2-one (B3) were presented in Figure 1. Their studied inhibitors concentration ranges are from 10^{-5} M to 5×10^{-3} M.
Prior all measurements, the mild steel samples (0, 13 % Cr ; 0.025 % Mo ; 0,26 % Si; 0.032 % Al; 0,16 % Cu; 0,13 % C and the remainder is iron) are abraded with a series of emery papers from 400 to 1200 grade. After

abrading the surface of specimens were rinsing with distilled water, degreasing in ethanol, and drying before use. Solution of 1 M HCl is prepared by dilution of analytical grade 37 % HCl with distilled water.

For weight loss measurements, rectangular mild steel specimens of size (4 cm ×1 cm × 0.05 cm) were used as samples for corrosion tests. After having been polished with emery paper and weighted, the samples were immersed for 24 h in 100 ml of uninhibited and inhibited solutions at room temperature in the air. At the end of immersion, the specimens were cleaned according to ASTM G-81 and reweighed to 10^{-4} g for determining corrosion rate [14]. The inhibition efficiency (η) is defined as follows:

$$\eta = \frac{\omega_{corr}^{0} - \omega_{corr}}{\omega_{corr}^{0}} \times 100 \qquad (1)$$

where ω^0_{corr} and ω are the corrosion rate values after immersion in solution without and with inhibitor, respectively.

For electrochemical measurements, a conventional three-electrode glass cell with a platinum counter electrode and a saturated calomel electrode (SCE) as reference was used. Mild steel cylindrical rod of the same composition as working electrode was pressure fitted into a polytetrafluoroethylene holder (PTFE) exposing only a 1 cm^2 surface to the solution. All tests were carried out at room temperature and in air atmosphere without bubbling. All potentials were measured against SCE.

The polarization curves were recorded by changing the electrode potential automatically with a Potentiostat/Galvanostat type PGZ 100, at a scan rate of 1 mV/s after its immersion in the test solution for 30 min until reaching steady state.

The evaluation of corrosion kinetics parameters was obtained using a non-linear regression calculation according to Stern–Geary equation:

$$i = i_{corr} \cdot \{exp[b_a \cdot (E - E_{corr})] - exp[bc \cdot (E - E_{corr})]\} \qquad (2)$$

where i_{corr} is the corrosion current density (A cm^{-2}), and b_a and b_c are respectively the Tafel constant of anodic and cathodic reactions (V^{-1}). These constants are related to the Tafel slope β (V/dec) in usual logarithmic scale by:

$$\beta = \frac{\ln(10)}{b} = \frac{2.303}{b} \qquad (3)$$

The inhibition efficiency was evaluated from the measured i_{corr} values using the relationship:

$$\eta = \frac{i_{corr}^{0} - i_{corr}}{i_{corr}^{0}} \times 100 \qquad (4)$$

where the superscript 0 indicates the corrosion current densities relative to that determined in the absence of inhibitor.

The electrochemical impedance spectroscopy measurements were carried out using a transfer function analyzer (VoltaLab PGZ 100), with a small amplitude ac. signal (10 mV rms), over a frequency domain from 100 KHz to 10 mHz. The results were then analyzed in terms of equivalent electrical circuit using Bouckamp program [15]. The inhibition efficiency has been found from the relationship:

$$\eta = \frac{R_{ct} - R_{ct}^{0}}{R_{ct}} \times 100 \qquad (5)$$

where R_{ct}^{0} and R_{ct} are the charge transfer resistance values in the absence and the presence of inhibitor, respectively.

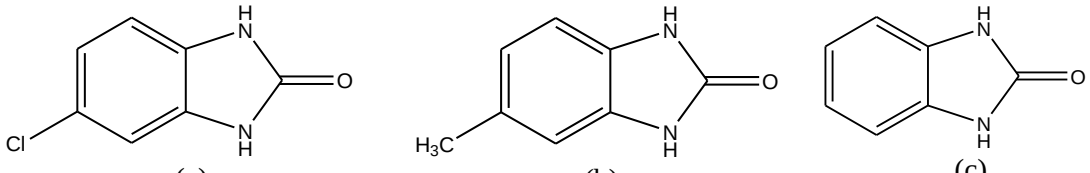

Figure 1: Molecular structure of the studied inhibitors: (a): 5-chloro-benzimidazol-2-one (B1), (b): 5-methyl-benzimidazol-2-one (B2) and (c): benzimidazol-2-one (B3)

3. Results and discussion:

3.1. Corrosion weight loss tests:

The benzimidazole derivatives effect on mild steel corrosion in 1 M HCl solution was studied using weight loss measurement after 24 h of immersion. The obtained results are presented in Table 1. It is noted that all compounds are a good corrosion inhibitor for mild steel in acidic media. As corrosion rate decreased, inhibition efficiency increased with increasing concentration and reaches a maximum at 10^{-3} M of B1.

The presence of B1 gives high inhibiting efficiencies and B3 somewhat lower efficiency. The difference in their inhibitive action can be explained by increasing of the effective electron density of the inhibitors by mesomeric effect in the case of –Cl in B1, and by inductive effect in the case of $–CH_3$ in B2 [3,16]. In aromatic or heterocyclic ring compounds, the effective electron density at the functional group can be varied by introducing different substituent in the ring, leading to variations of the molecular structure.

Table 1: Inhibition efficiency for various benzimidazole derivatives compounds of mild steel in 1 M HCl obtained from weight loss measurements after 24 h of immersion

Compounds	C (M)	w_{corr} (mg/cm^2 h)	θ	η (%)
00	00	0.102	-	-
B1	10^{-5}	0,044	0.5686	57
	10^{-4}	0,043	0.5784	58
	5×10^{-4}	0,031	0.6960	70
	10^{-3}	0,013	0.8712	87
B2	10^{-3}	0,031	0.6960	70
B3	10^{-3}	0,085	0.1667	17

Generally, inhibitors may function by physisorption, chemisorptions or by complexation with metal ions. The adsorption isotherm type can provide additional information about the properties of tested compounds. However, the coverage surface (θ) can be easily determined from ac impedance, polarization or weight loss measurements by the ratio $\eta/100$.

In this study, the coverage surface is estimated from weight loss measurements to make the fitting and select the suitable isotherm. The following adsorption isotherms are the most common models to study the mechanism of corrosion inhibition [17, 18]:

Tempkin adsorption isotherm $$\exp(f\times\theta) = K_{ads}\times C_{inh} \quad (6)$$

Langmuir adsorption isotherm $$\frac{\theta}{1-\theta} = K_{ads}\times C_{inh} \quad (7)$$

Frumkin adsorption isotherm $$\frac{\theta}{1-\theta}\exp(-2\times f\times\theta) = K_{ads}\times C_{inh} \quad (8)$$

Freundlich adsorption isotherm $$\theta = K_{ads}\times C_{inh} \quad (9)$$

Flory–Huggins adsorption isotherm $$\log(\frac{\theta}{C_{inh}}) = \log(K_{ads}) + a\times\log(1-\theta) \quad (10)$$

where K_{ads} is the equilibrium constant of the adsorption process, C_{inh} is the inhibitor concentration, f is the factor of energetic inhomogeneity and the parameter 'a' in Eq. (10) is the number of water molecules replaced by inhibitor molecules on metal surface.

For each inhibitor, a Tempkin, Langmuir, Frumkin, Freundlich and Flory–Huggins isotherm were fitted. Table 2 shows the corresponding fitting curve results where r^2 is the square of the correlation coefficient between the dependent variables and the estimated values by the regressors, or equivalently defined as the ratio of regression variance to total variance. It is seen that the best fit shows that the inhibitors are adsorbed on metallic surface according to the Langmuir isotherm model. In addition, Figure 2 shows the relationship between C_{inh}/θ and C_{inh}

(Langmuir isotherm) for the best inhibitor (B1). From the intercepts of the straight lines C_{inh}/θ vs. C_{inh}, the equilibrium constant values of the adsorption process, K_{ads} can be determined. This constant is related to the free energy of adsorption, ΔG^0_{ads}, by the following equation [19]:

$$K_{ads} = \frac{1}{55,55}\exp(-\frac{\Delta G^0_{ads}}{RT}) \qquad (11)$$

where 55,55 value represents the water concentration in solution by mol L^{-1}, R is the universal gas constant and T is the absolute temperature.

The free energy of adsorption, ΔG^0_{ads} can be calculated. It is well known that ΔG^0_{ads} values on the order of - 20 kJ mol^{-1} or less indicate a physisorption, while those more negative than - 40 kJ mol^{-1} involve charge sharing or transfer from the inhibitor molecules to the metal surface to form a coordinate chemical bond (chemisorptions), while values between -20 kJ mol^{-1} and - 40 kJ mol^{-1} indicate both physisorption and chemisorption [20]. In our case, ΔG^0_{ads} values of B1 is -34.38 kJ mol^{-1}. This value indicated that adsorption of B1 occurs via both chemisorption and physisorption [21, 22].

Table 2: Curve fitting results of inhibitors for different adsorption isotherms.

Adsorption isotherms types	Temkin	Langmuir	Frumkin	Freundlich	Flory–Huggins
Linear coefficient regression	0.8386	0.9917	0.8141	0.85796	0.5779
ln K_{ads} (M^{-1})	1.187	9.79	5.8462	0.3326	-19617.36

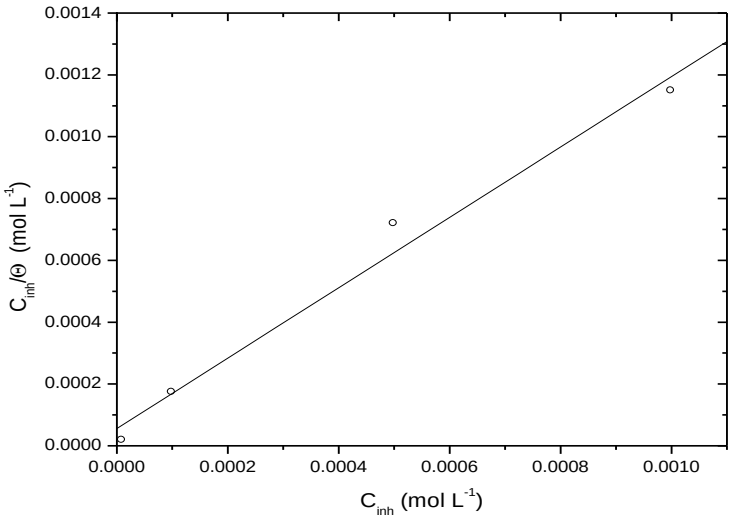

Figure 2: The relationship between C_{inh}/θ and C_{inh} for different inhibitors

3.2. Potentiodynamic polarization curves:

In the previous part, we noted that the B1 is the best inhibitor. In fact, we studied its effect on the mild steel corrosion in acidic medium. Figure 3 depicts typical potentiodynamic polarization curves of B1 at different concentration on mild steel in 1 M HCl. It is noted that the anodic branches do not show any linearity due to the metal dissolution. For this, i_{corr}, E_{corr}, b_a and b_c were evaluated from the experimental results using a user defined function of "Non-linear least squares curve fit" (using Eq. (2)) of graphic software (Origin, Origin Lab). In all cases, the correlation factor R^2 is greater than 0.999 indicating a reliable result. Figure 4 shows, as for an example, the results of regressions calculation for the cathodic and anodic scan in the presence of B1 at various concentrations. In this calculation, the potential domain is limited to E_{corr} ± 0.100 V/SCE such as mentioned in our previous work [6]. It can be seen in this figure a good agreement between the calculated and the experimental polarization data. Table 3 summarizes various corrosion kinetic parameters so obtained. It is can be remarked that the current density values decrease with concentration. In other hand, The cathodic Tafel slope (b_c), relating to the polarization of mild steel in 1M HCl, is equal to -112 mV dec^{-1} (20.44 V^{-1}). As reported in the literature [23], this value indicates, in general, that the reduction reaction of hydrogen on iron takes place according to the mechanism of Volmer-Heyrovsky:

$$H^+_{ads} + e^- \rightarrow H_{ads} \quad (12)$$
$$H_{ads} + H^+ + e^- \rightarrow H_2 \quad (13)$$

In the presence of inhibitor, the b_c values change with B1 addition, but this necessarily does not result from a modification of the reaction mechanism [24]. Indeed, when the coverage rate increases with increasing inhibitor concentration, the electrode active surface is reduced and the adsorbed film can have an ohmic behaviour, which appears by an increase in the b_c value [25].

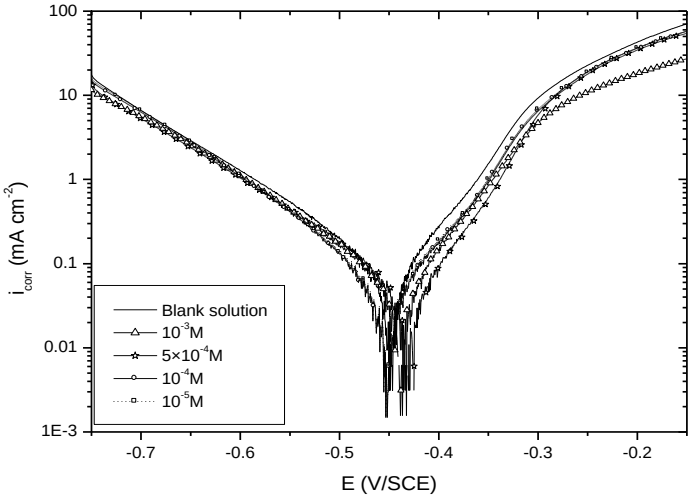

Figure 3: Potentiodynamic polarization curves for mild steel in 1 M HCl at different concentration of B1 at room temperature

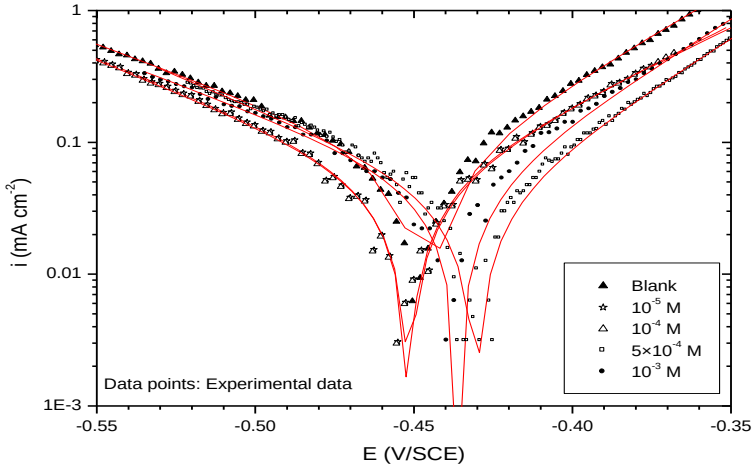

Figure 4: Comparison of experimental and fitting data using a non-linear fitting with Stern-Geary equation of mild steel in 1 M HCl in the presence of B1 at different concentration

Table 3: Electrochemical parameters for mild steel in 1 M HCl containing different concentration of B1 at room temperature.

C (M)	E_{corr} (mV/SCE)	b_a (V^{-1})	b_c (V^{-1})	i_{corr} (µA cm^{-2})	η (%)
00	-446	32.05	-20.44	166.68	-
10^{-5}	-451	26.42	-21.85	50.60	70
10^{-4}	-451	27.51	-22.10	47.78	71
5×10^{-4}	-436	34.77	-20.97	43.42	74
10^{-3}	-430	37.37	-23.18	35.99	78

3.3. Electrochemical impedance spectroscopy (EIS):

The corrosion behavior of mild steel in 1M HCl solution for different concentration of B1, was investigated using EIS method at room temperature after 1h of immersion at corrosion potential (Figure 5). In order to obtain more mechanistic information on inhibition mechanism an equivalent electrical circuit (Figure 6) was utilized. After fitting experimental data to the equivalent, electrical circuit solution resistance (R_s), charge transfer resistance (R_{ct}) and constant phase element (Q_{ct}) were determined. This circuit has been used previously to model the iron-acid surface [26]. It is apparent from these plots that the impedance response of mild steel in uninhibited 1 M HCl solution has significantly changed after B1 addition. It's higher for 10^{-3} M of B1. In addition, the presented impedance spectra take the form of characteristic capacitive semi-circles that correspond to one time constant. In order to gain more detailed information on adsorption mechanism of B1, impedance data were analyzed using this appropriate equivalent electrical circuit (Figure 6).

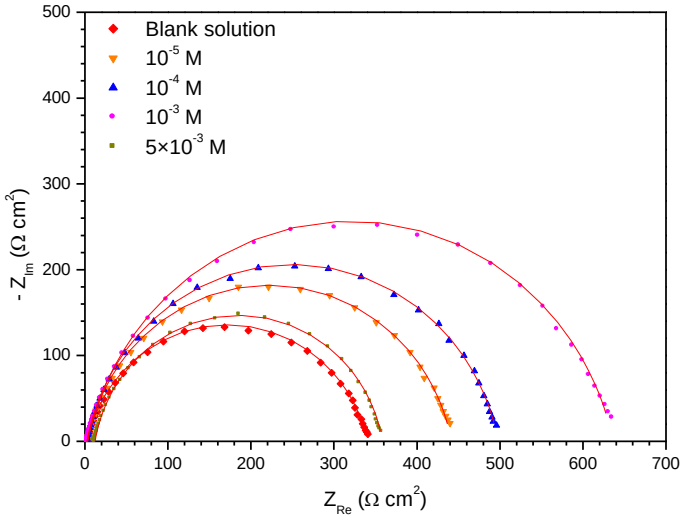

Figure 5: Nyquist plots for mild steel in 1 M HCl containing different concentrations of B1 at room temperature (Symbols: Experimental data and Lines : Fitting data)

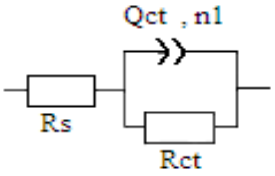

Figure 6: Equivalent circuit model used to fit the experiment impedance data for the metal-acid interface

It is worth pointing out that application of an electrical circuit consisting of double layer capacitor does not always enable achieving satisfactory fitting to the experimental impedance data. The Nyquist plot represents time constant (or frequency) dispersion of the impedance data. It can be attributed to the rough and inhomogenous surface onto which the B1 was adsorbed. In such case using an equivalent electrical circuit employing the double layer capacitance element is not a good enough approximation. Assuming surface heterogeneity a modeling element with frequency dispersion behavior known as Constant Phase Element (CPE) was suggested instead of C_{dl}. The CPE behavior can be attributed to surface heterogeneity resulting from the inhibitor's adsorption (mainly), surface roughness, dislocations, impurities, grain boundaries, fractality, etc. The more heterogenous surface, hence the higher n values, the greater deviation from ideal capacitative behavior. Thus it allows employing CPE element in order to investigate efficiency and the properties of the inhibitive film on the metal surface. An electrical equivalent circuit R(QR) where Q stands for CPE employed in this work has been reported [27–**29**]. Figure 7 demonstrates constant phase element (Q) and n values as a function of various B1 concentrations. It is noticeable that the decrease in Q values at 10^{-4} and 10^{-3} M of B1 which is associated with an increase in n values. The impedance of CPE can be described by equation below:

$$Z_{CPE} = \left[Q(j\omega)^n \right]^{-1} \quad (14)$$

where j is the imaginary number, Q is the frequency independent real constant, ω = 2πf is the angular frequency (rad/s), f is the frequency of the applied signal, n is the CPE exponent for whole number of n = 1, 0, -1, CPE is reduced to the classical lump element-capacitor (C), resistance (R) and inductance (L) [30].

The employment of Q and n parameter is justified in case their changes are related to the surface heterogeneity. In general the role of the inhibitor is to form an efficient barrier against aggressive ions and adsorb on the most active adsorption sites. In this investigation the inhibition effect of B1 was revealed by changes of R_{ct}, n and Q parameters. The higher R_{ct} values that increase simultaneously with the concentration of B1, the greater the mild steel surface covered with inhibitive film.

Figure 7 shows that the n value increases with the increase of B1 concentration. A reason for that might be due to the decrease of surface heterogeneity as a result of the adsorption of B1 molecules on the mild steel surface and forming a uniform inhibitive film. Simultaneously the values of Q decrease on the addition of higher concentrations of B1. Water molecules that are present on metal/solution interface possess a higher value of the relative dielectric constant. When water molecules are replaced by inhibitor molecules, a decrease on the value of Q occurs [31,32].

However, the electrochemical parameters derived from the Nyquist plots and inhibition efficiencies values are given in Table 4. For all concentration of B1, the charge transfer resistance increase comparing to blank solution. This change can result from a decrease in local dielectric constant and/or an increase in the thickness of the electrical double layer suggests that the inhibitors molecules function by adsorption at the metal–solution interface [33]. The adsorption of this product on electrode surface displaces the water molecule and other ions already adsorbed such as mentioned above. EIS impedance study also confirms the inhibition character of B1 obtained with gravimetric and polarization curves measurements.

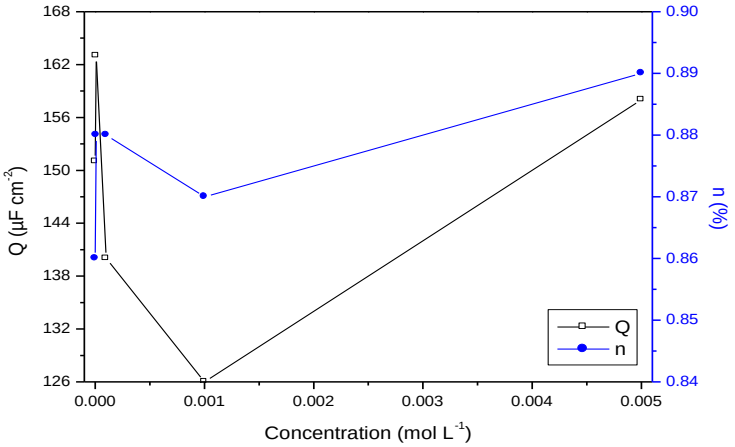

Figure 7: Constant phase element Q and n parameters in a function of concentration of B1.

Table 4: Data obtained from EIS measurements for mild steel in 1 M HCl in the presence of different concentrations of B1.

C (M)	R_s (Ω cm^2)	R_{ct} (Ω cm^2)	Q (µF cm^{-2})	n	η (%)
0	2.47	338	151	0.86	-
10^{-5}	3	438.5	163	0.88	23
10^{-4}	2.53	495.1	140	0.88	32
10^{-3}	1.15	633.1	126	0.87	47
5×10^{-3}	12.27	346.1	158	0.89	03

3.4. Immersion time:

Figure 8 shows the impedance spectra for mild steel in 1 M HCl at different immersion times in the presence of B1 at the optimum concentration. It is noted that these diagrams exhibit one capacitive loop for the immersion time range from 1/4 h to 4 h which its diameter increases with immersion time. At 24 h, the diagram exhibit two

loops, the first was attributed the film formation while the second was attributed to capacitive behavior. In order to obtain more mechanistic information of corrosion inhibition, the same equivalent electrical circuit (Figure 6) was proposed for the immersion time range from 1/4 h to 4 h while for 24 h another equivalent circuit (Figure 9) was utilized. After fitting experimental data to the equivalent, electrical circuit solution resistance (R_s), film formation resistance (R_f), constant phase element of the formed film (Q_f), charge transfer resistance (R_{ct}) and constant phase element (Q_{ct}) were determined. At 24h, it is noted the apparition of a proactive film by B1 molecules.

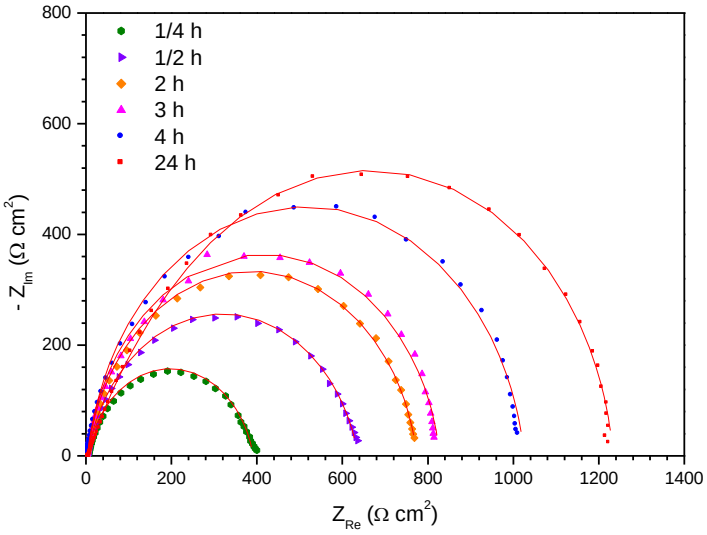

Figure 8: Nyquist diagrams for mild steel in 1 M HCl containing 10^{-3} M of B1 at different immersion time over open circuit potential (Symbols: Experimental data and Lines : Fitting data).

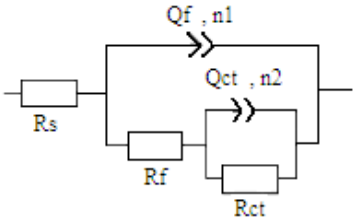

Figure 9: Equivalent circuit model used to fit the experiment impedance data for the metal-acid interface (For 24 h of immersion time)

Table 5: Influence of immersion time on the electrochemical parameters for mild steel in 1 M HCl in the presence of 10^{-3} M of B1.

Immersion time (h)	R_S (Ω cm^2)	R_f (Ω cm^2)	Q_f (μF cm^{-2})	n_1	R_{ct} (Ω cm^2)	Q_{ct} (μF cm^{-2})	n_2	η (%)
1/4	1.85	-	-	-	388.1	166	0.87	13
1/2	1.15	-	-	-	633.1	126	0.87	47
2	3.82	-	-	-	770.2	99.33	0.91	56
3	3.66	-	-	-	823.9	85.7	0.92	59
4	4.76	-	-	-	1021	65.56	0.92	67
24	11.21	236.7	17.76	0.99	988.4	48.67	0.93	72

The evolution of the characteristics parameters associated with the capacitive loop with time is summarized in Table 5. It is remarked that the R_{ct} values increased when Q_{ct} values decreased with increasing of immersion time. The decrease in the Q_{ct} which can result from a decrease in local dielectric constant and/or an increase in the thickness of the double layer was attributed to the inhibitor molecules adsorption on the metal surface [34].

However, it is known that in acidic media the halide ions facilitate the adsorption of organic inhibitors through intermediate bridges between metal surface and positively charged inhibitor. Thus, if the inhibiting effect is due to the protonated species, a synergistic increase in inhibition efficiency should be observed in the presence of the halide ions [35]. These results indicate that the immersion time increases the chlorides quantity which will be adsorbed on the surface helping to the inhibitor layer formation. This increase indicate a formation of compact film, therefore the B1 adsorption, on the electrode surface is reinforced with immersion time and is relatively fast and completed within ca. two hours. In addition, these results indicate that the adsorption model, arrangement and orientation of B1 on metallic surface, change with time [33].

3.5. Mechanism action:

The organic cations have the same adsorption centers which are the –NH– groups (protonated form $–NH_2^+–$) and the de-localized π-electrons of heterocyclic ring. In addition, this compound can be protonated in acid medium. Thus, it becomes cations, existing in equilibrium with their corresponding molecular form:

$$B_1 + xH^+ \leftrightarrow \left[B_1H_x\right]^{x+} \quad (15)$$

However, the investigated compound can be classified as: the electrolytes, the protonated products being the cations and the inorganic parts present in solution (Cl^-) being the anion. The effectiveness of this inhibitor can be explained by assuming the adsorption process as the cause of inhibition. The B1 can be regarded as a dipole species, the ternary $–NH_2^+–$ groups is the positive side, while the de-localized π-electrons of the substituted phenyl ring is the negative side of the dipole, where the B1 has only the quaternary $–NH_2^+–$ groups. Accordingly, the inhibition by such dipoles may be stabilized by the participation of tow mode of adsorption as follows: (1) Electrostatic interaction (physisorption) between the positively charged $–NH_2^+–$ groups and the negatively charged mild steel surface [36]. (2) Interaction between the outermost negative end of the dipole (de-localized π –electrons of the substituted phenyl ring) and the vacant, low energy d-orbitals of Fe surface atoms (chemisorptions). The former (physisorption) is enhanced by the co-adsorption of Cl^- ions [37, 38], while the latter (chemisorption) is run parallel to the ‘‘electron donor property’’ of the substituent type and the electron availability.

Armaki et al. [39] pointed that the amine type inhibitors, inhibit both the anodic and cathodic processes of metal in acidic solution. In the anodic region the non-protonated amines are chemisorbed on metal surface through the interaction between the lone pair of nitrogen atom and the metal atom, while in the cathodic region, the onium ions formed in acidic solution are adsorbed on the negatively charged surface, by electrostatic interaction with the metal.

On the other hand, increasing inhibitor concentration leads to mutual stimulation of adsorption between the $–NH_2^+–$ groups and the Cl^- anions [40]; thus physisorption is predominant. Here, it is abundant of protonated inhibitor on mild steel surface, accordingly steric effect becomes more pronounce, leading to decrease the possibility of adsorption through chemisorption mechanism. Moreover, Cl^- ions play an essential role in reducing the repulsive forces between the ammonium groups and hence stabilizing the physisorption, so a closed packed layer at the metal surface may be formed [41].

Conclusion:

From the above results and discussions, the following conclusions are drawn:

1. The obtained results show that the benzimidazoles have a limited corrosion inhibition for mild steel in 1 M HCl due to their protonation so the B1 is the better.
2. B1 is adsorbed on metallic surface according to Langmuir isotherm model.
3. The inhibition efficiency of B1 can be stabilized by the participation of tow adsorption mode (physisorption and chemisorption).
4. At 24 h of immersion, the EIS study showed the formation of a protective film.
5. Reasonably good agreement was observed between the obtained data from weight loss measurement, potentiodynamic polarization curves and electrochemical impedance spectroscopy techniques for the B1.

References

1. Zarrok H., Oudda H., El Midaoui A., Zarrouk A., Hammouti B., Ebn Touhami M., Attayibat A., Radi S., Touzani R., *Res. Chem. Intermed.*, 38 (2012) 2051.
2. Zerga B., Hammouti B., Ebn Touhami M., Touir R., Taleb M., Sfaira M., Bennajeh M., Forssal I., *Int. J. Electrochem. Sci.*, 7 (2012) 471

3. Elkacimi Y., Achnin M., Aouine Y., Ebn Touhami M., Alami A., Touir R., Sfaira M., Chebabe D., Elachqar A., Hammouti B., *Portugaliae Electrochim. Acta,* 30 (2012) 53-65.
4. Aouine Y., Sfaira M., Ebn Touhami M., Alami A., Hammouti B., Elbakri M., El Hallaoui A., Touir R., *Int. J. Electrochem. Sci.*, 7 (2012) 5400.
5. Zarrouk A., Zarrok H., Salghi R., Hammouti B., Bentiss F., Touir R., Bouachrine M., *J. Mater. Environ. Sci.*, 4 (2013) 177.
6. Benbouya K., Forsal I., Elbakri M., Anik T., Touir R., Bennajah M., Chebab D., Rochdi A., Mernari B., Ebn Touhami M., *Res. Chem. Intermed.,* (2012) DOI 10.1007/s11164-013-1037-z
7. Aderdour K., Touir R., Ebn Touhami M., Sfaira M., El Kafssaoui H., Hammouti B., Benzaid H., Essassi E. M., *Der Pharma Chemica,* 4 (2012) 1485-1495
8. Ehteshamzade M., Shahrabi T., Hosseini M.G., *Appl. Surf. Sci.*, 252 (2006) 2949.
9. Lebrini M., Bentiss F., Vezin H., Lagrenée M., *Corros. Sci.*, 48, (2006) 1279.
10. Elbakri M., Touir R., Ebn Touhami M., Zarrouk A., Aouine Y., Sfaira M., Bouachrine M., Alami A., El Hallaoui A., *Res. Chem. Intermed.,* 39 (2013) 2417
11. Hmimou J., Rochdi A., Touir R., Ebn Touhami M., Rifi E. H., El Hallaoui A., Anouar A., Chebab D., *J. Mater. Environ. Sci.*, 3 (2012) 543-550.
12. Galal A., Atta N. F., Al-Hassan M. H. S., *Mater. Chem. Phys.*, 89 (2005) 38.
13. Bentiss F., Gassama F., Barbry D., Gengembre L., Vezin H., Lagrenée M., Traisnel M., *Appl. Surf. Sci.*, 252 (2006) 2684.
14. ASTM G-81, Annual Book of ASTM Standards, (1995).
15. Bouckamp A., Users Manual Equivalent Circuit, Ver. 4.51, (1993).
16. Wang R. H. L., Liu R.-B., Xin J., *Corros. Sci.,* 46 (2004) 2455.
17. Abiola O. K., *Corros. Sci.*, 48 (10) (2006) 3078-3090.
18. Oguzie E. E., *Corros. Sci.* 49 (3) (2007) 1527- 1539.
19. Khamis E., Bellucci F., Latanision R. M., El-Ashry E. S. H., *Corrosion* 47 (1991) 677-686.
20. Kustu C., Emregul K. C., Atakol O., *Corros. Sci.*, 49 (2007) 2800- 2814.
21. Li W., He Q., Pei C., Hou B., *Electrochim. Acta,* 52 (2007) 6386-6394.
22. Ammar I. A., El Khorafi F. M., *Werkst. Korros.*, 24 (1973) 702-707.
23. Adardour K., Kassou O., Touir R., Ebn Touhami M., ElKafsaoui H., Benzeid H., Essassi E. M., Sfaira M., *J. Mater. Environ. Sci.*, 1 (2) (2010) 129-138.
24. Pillai K. C., Narayan R., *Corros. Sci.*, 23 (1983) 151-166.
25. Vijh A. K., Conway B. E., *Chem. Rev.*, 67 (1967) 623-664.
26. Cissé M., Abouchane M., Anik T., Himm K., Belakhmima R. A., Ebn Touhami M., Touir R., Amiar A., *Inter. J. Corros.*, volume 2010, article ID 246908 , doi:10.1155/2010/246908
27. Bentiss F., Lebrini M., Vezin H., Chai F., Traisnel M., Lagrenée M., *Corros. Sci*., 51 (2009) 2165.
28. Popova A., Raicheva S., Sokolova E., Christov M., Langmuir 12 (1996) 2083.
29. López D.A., Simison S.N., *Electrochim. Acta*, 48 (2003) 845.
30. Gerengi H., Darowicki K., Bereket G., Slepski P., *Corros. Sci.*, 51 (2009) 2573.
31. Souza F.S., Spinneli, A., *Corros. Sci*., 51 (2009) 642
32. Gerengi H., Schaefer K., Ibrahim Sahin H., *J. Indust. Eng. Chem.*, 18 (2012) 2204–2210
33. Touir R., Dkhireche N., Ebn Touhami M., Sfaira M., Senhaji O., Robin J. J., Boutevin B., Cherkaoui M., *Mater. Chem. Phys.*, 122 (2010) 1–9.
34. Babic-Samardzija K., Khaled K. F., Hackerman N., Anti-Corros., Method Mater., 52 (2005)11.
35. Oguzie E., Li Y., Wang F. H., *J. Colloid Interface Sci.*, 310 (2007) 90.
36. Bentiss F., Traisnel M., Lagrenée M., *Corros. Sci.*, 42 (2000) 127-146.
37. Driver R., Meakins R. J., *Br. Corros. J.*, 12 (1977) 46-50.
38. Subramaniam G., Balasubramanian K., Sridhar P., *Bull. Electrochem.*, 6(1990) 225-229.
39. Aramaki K., Kagaku D., 41 (1973) 875 in: Willars M., Hampson N. A., *Surf. Technology*, 4 (1976) 465.
40. Quraishi M. A., Rawat J., *Mater. Chem. Phys.*, 73 (2002) 118-122.
41. Frignani A., Trabanelli G., Zucchi F., Zucchini M., in: Proceeding of the 5th European Symposium on Corrosion Inhibitors, Ann. Univ., Ferrara, (1980).